MRS Advances © 2017 Materials Research Society
DOI: 10.1557/adv.2017.488

Investigation of charge transport between nickel oxide nanoparticles and CdSe/ZnS alloyed nanocrystals

R. Vasan*[1], F. Gao[2], M. O. Manasreh[1], C. D. Heyes[2]
[1]Department of Electrical Engineering, University of Arkansas, Fayetteville, AR, USA-72701
[2]Department of Chemistry and BioChemistry, University of Arkansas, Fayetteville, AR, USA-72701

ABSTRACT

Charge transport between nickel oxide nanoparticles and CdSe/ZnS alloyed core/shell nanocrystals is investigated. The crystal structure and composition of the nickel oxide nanoparticles are evaluated using X-ray diffraction, Raman and X-ray photoelectron spectroscopies. The nanoparticles are near-stoichiometric with very low defect densities. The optical properties of the materials are studied by measuring the absorbance and time resolved photoluminescence spectra. The band gap of the nickel oxide nanoparticles is around 4.42 eV. The CdSe/ZnS nanocrystals exhibit shorter average lifetimes when mixed with nickel oxide nanoparticle powder. The lifetime quenching can be attributed to the efficient charge transport from the CdSe/ZnS nanocrystals to nickel oxide nanoparticles due to the relative valence band alignment.

INTRODUCTION

Recently inorganic colloidal quantum dots (QDs) were investigated as a replacement for existing organic active layers in photovoltaic devices and organic light emitting devices. One of the main reasons for this change is the environmental stability and high current operation of these devices with inorganic QDs [1]. The most commonly employed QDs are colloidally grown CdSe/ZnS and CdSe/CdS core-shell nanocrystals. Even though an alternative inorganic active material is employed, these devices still use organic charge transport layers [1]. The charge transport layers facilitate the extraction of carriers in photovoltaic devices and injection of carriers in light emitting devices. In the case of light emitting devices, the charge transport layers reduce the barrier to holes and electrons that are injected from the electrode into the QD emissive layer [2-4]. Suitable inorganic electron transport layers reported so far are zinc oxide, titanium dioxide, and tin oxide, which are intrinsically n-type materials [1-4]. The conduction band of the electron transport layers align with the conduction band of the QD and thereby reduce the barrier to electrons injected from the cathode, but there are not enough hole transport layers (HTLs) with suitable valence band alignment with the QDs. Even though some p-type materials are used as HTLs, the efficiency of the devices is much lower due to valence band mismatch [1, 2-4]. Non-stoichiometric nickel oxide (NiO) has been successfully employed as an HTL in quantum light emitting devices (QLEDs), but imbalance in the charge injection into the QDs created by the high barrier to holes resulted in low efficiency [2-4].

In this study, near-stoichiometric NiO nanoparticles are synthesized and characterized for application as a potential HTL for all-inorganic QLEDs. The structural and compositional studies of the synthesized nanoparticles indicate that the formed material is near-stoichiometric with very low defect densities. The synthesis process is controlled such that the bandgap of the nanoparticles is very high on the order of 4.4 eV and the valence band maximum is ~6.2 eV below the vacuum level. This makes the NiO nanoparticles a suitable material for hole injection into the CdSe/ZnS alloyed core shell QDs. The charge transport mechanism between NiO nanoparticles and the QDs is investigated by measuring the lifetimes of QDs mixed with an

equal weight ratio of NiO nanoparticles. The lifetime of QDs are quenched when mixed with the nanoparticles and is an indication of effective charge transport between the two materials. This is further bolstered by QD size dependency of the lifetime quenching. In order words, the lifetimes of QDs with a wider bandgap are quenched more than the lifetimes narrow band gap QDs, due to the low valence band mismatch between the wide band gap QDs and the NiO nanoparticles.

EXPERIMENT

Nickel oxide nanoparticles were synthesized by the hydrolysis of nickel acetate solution. Initially, 0.5 M solution of nickel acetate was formed by dissolving the salt in 10 ml of DI water. 1.0 M solution of sodium hydroxide in DI water was added dropwise over 10 mins. The bright green clear solution became turbid and formed a pale green precipitate. The resulting nickel hydroxide precipitate was then washed twice with DI water and centrifuged to collect the precipitate. The precipitate was first dried under vacuum and ground to a fine powder. The ground powder was then annealed at 360 ^{o}C for 2 hrs under ambient air inside a box furnace forming a black powder of NiO nanoparticles. Nickel oxide nanoparticles were then dispersed in DI water for further experiments.

The core/shell nanocrystals were synthesized by modifying the procedure reported by Bae *et. al* [5]. In a typical single step synthesis, 0.1 mmol of cadmium oxide and 4 mmol of zinc acetate were heated with 5ml of oleic acid in a three neck round bottom flask. The mixture was degassed at 150 ^{o}C for 30 min to remove any volatile impurities. After degassing, 15 ml of octadecene was injected into the flask and the temperature was increased. At 300 ^{o}C, 2ml of trioctylphosphine dissolving 0.2 mmol of Se and 3 mmol of S was injected rapidly into the reactor. The reaction was allowed to continue for 10 min before the reactor was rapidly cooled down to room temperature. The resulting nanocrystals were purified by precipitating with excessive methanol and hexane. The purification process was repeated at least 3 times before the nanocrystals were dried and dispersed in hexane at 25 mg/ml concentration for further experiments. The starting precursor ratio yielded green emitting (533 nm) nanocrystals with a FWHM of 29 nm. By keeping the synthesis temperature, time, and ligand concentration constant, the starting precursor ratio was changed to obtain the blue and orange emitting QDs.

Fluorescence lifetimes were measured using a MicroTime 200 scanning confocal fluorescence microscope (PicoQuant GmbH, Berlin, Germany), which is based on Olympus IX71 equipped with PicoHarp 300 TCSPC controller [6-8]. It utilizes a 485 nm laser (PDL 485, Picoquant) operating in pulsed wave mode at a power of ~0.05 μW and repetition rate of 4 MHz for excitation of QD samples. A dichroic mirror (500dcxr, Chroma, McHenry, IL) sends the light through a water immersion objective (Olympus, Apochromat 60x, NA 1.3) to a diffraction-limited laser focus. The absorption spectra of the materials were recorded using a Cary 500 UV-Vis spectrophotometer. The Raman spectrum was measured using a LabRam Micro Raman/PL measurement system with an excitation wavelength of 473 nm and a Si CCD detector.

RESULTS AND DISCUSSION

The structural and compositional properties of the NiO nanoparticles are characterized by XRD, Raman and XPS measurements. The grazing angle XRD scan of the NiO nanoparticle powder is shown in Fig. 1(a). The diffracting planes (111), (200), (220), (311), and (222) located at 37.2^{o}, 43.27^{o}, 62.8^{o}, 75.3^{o}, and 79.3^{o} respectively, are characteristic of NiO rock salt structure. The reference indices for bunsenite structure from JCPDS card no: 01-075-0197 are also marked in Fig. 1(a). The crystallite size, as calculated from Scherrer's equation, is 5 – 6 nm indicating

that the formed NiO is nanocrystalline. NiO thin films and nanoparticles reported so far are non-stoichiometric with nickel vacancies [9, 10]. Presence of these defects are identified by the shift in the diffraction peaks, specifically the (200) and (220) planes, when compared to stoichiometric NiO or bunsenite [9]. The NiO nanoparticles reported here are near-stoichiometric with fewer defects as the diffraction planes exactly align with the bunsenite reference indices. This can also be seen in the Raman spectrum of the NiO nanoparticles shown in Fig. 1(b). The LO phonon mode at 510 cm^{-1} is characteristic of near-stoichiometric NiO. This mode is shifted to 560 cm^{-1}, when the NiO is formed in an oxygen rich environment leading to the formation of nickel vacancies, which makes the final NiO non-stoichiometric [11]. The composition of the NiO nanoparticles is determined by XPS measurements. A survey of the material indicates the presence of nickel, oxygen and carbon. The carbon is from the nickel acetate, which is the precursor. The detailed XPS spectrum for the Ni2p3/2 state is shown in Fig. 2(b). The original spectrum is fitted with three Gaussian peaks. The peak centered at 854.2 eV binding energy corresponds to the Ni^{2+} oxidation state of Ni from stoichiometric NiO. The higher binding energy peak at 856.0 eV corresponds to the Ni^{3+} oxidation state, which is a result of non-stoichiometric Ni_2O_3 or NiOOH formed due to nickel vacancies [9, 10]. Finally, the peak at 861 eV is due to the shake up process [9]. Figure 2 (c) shows the XPS spectrum O1s state. The peaks at 529.1 eV and 530.98 eV correspond to NiO and Ni_2O_3 or NiOOH respectively [9, 10]. The composition ratio of Ni^{2+} to Ni^{3+} is 1:1.7, which is much lower than the ratio for NiO thin film [9, 10]. All the above results show that the formed NiO nanoparticles are near-stoichiometric.

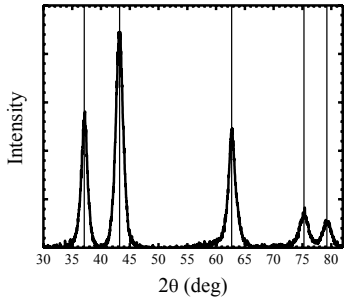

(a)

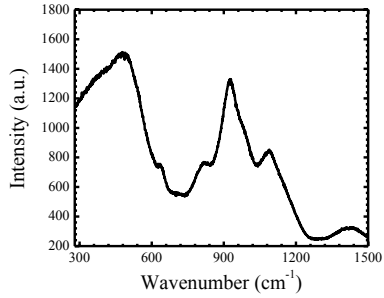

(b)

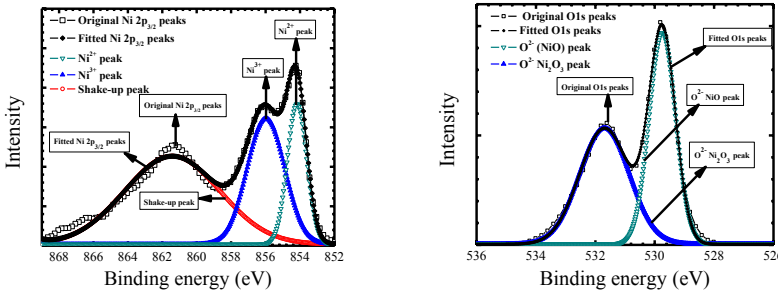

(c) (d)

Figure 1. (a) The crystallinity of solution processed near-stoichiometric NiO nanoparticles is determined from the XRD measurement. The diffracting planes (111), (200), (220), (311), and (222) of NiO nanoparticles are indexed and compared to the bunsenite or stoichiometric NiO (JCPDS card no: 01-075-0197). **(b)** Raman spectrum of NiO nanoparticles grown by oxidation of $Ni(OH)_2$. The composition of the NiO HTL is measured from the integral area of **(c)** Ni peaks of Ni2p3/2 and **(d)** O peaks of O1s curves from the XPS spectrum of NiO.

The optical properties of NiO nanoparticles and the QDs are investigated by measuring the absorbance and time-resolved PL spectroscopies. The absorbance of NiO nanoparticles is shown in Fig. 2(a). The band gap of the synthesized near-stoichiometric NiO nanoparticles as calculated from the excitonic peak in Fig. 2 (a) is 4.42 eV. This band gap value is much higher than the reported band gap of non-stoichiometric NiO [2-4, 9, and 10]. The charge transport between the near-stoichiometric NiO nanoparticle HTL and the QDs is investigated by time-resolved PL measurements. The blue, green and orange QDs in hexane are each mixed separately with equal amount of NiO nanoparticle powder and the average lifetimes are measured. As control samples, the average lifetimes of as-prepared QDs dispersed in hexane are also measured. Figure 2. (b), Fig. 2 (c), and Fig. 2 (d) show the decay curves of QDs mixed with NiO compared to the control samples. The average lifetimes of blue, green and orange QDs in hexane are 17.01 ns, 20.82 ns and 31.67 ns, respectively. It can be noted that the lifetimes of QDs when mixed with NiO nanoparticles are quenched significantly and that the quenching is dependent on the size of the QD. The lifetime of blue QDs quench the highest, followed by green and orange QDs. Normally, QD lifetime quenching is encountered in QD films due to self-quenching effects. In this case, the QDs are still well dispersed in hexane and the lifetime quenching can be attributed to efficient hole transport from the QDs into the NiO nanoparticles.

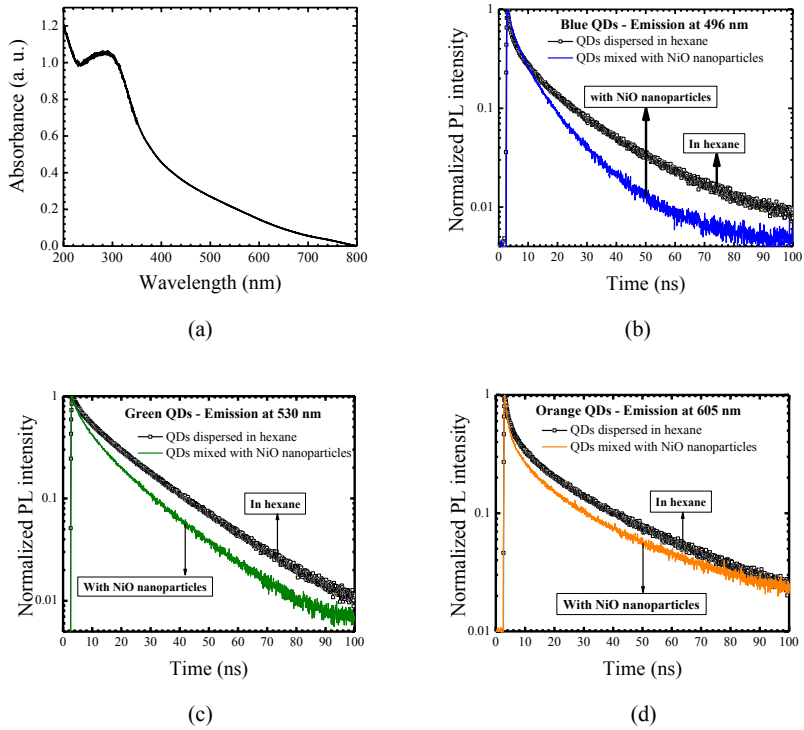

Figure 2. (a) The band gap of the NiO nanoparticles is calculated from the excitonic peak of the absorbance spectrum. The lifetime of **(b)** 496 nm, **(c)** 530 nm and **(d)** 605 nm emitting CdSe/ZnS QDs shortened when mixed with the NiO nanoparticles, which indicates an efficient charge transport between the two materials. The lifetimes of control samples are plotted as a symbol plot and QDs mixed with NiO nanoparticles are plotted using a line plot.

The study shows that the QDs exhibit a strong interaction with the NiO nanoparticle powder. The NiO nanoparticles reported here are near-stoichiometric with a wide band gap of ~4.4 eV and a deep valence band maximum at -6.22 eV. The valence band value is calculated from the reported electron affinity value for NiO [2-4]. It can be seen that the lifetime of QDs is quenched significantly when mixed with the NiO nanoparticles. Also, lifetime quenching increases with an increase in the band gap of the QDs. In other words, quenching is dependent on the relative valence band alignment of the QDs with NiO nanoparticles. The valence band of blue QDs aligns well with the NiO nanoparticles, leading to 41% quenching in lifetime. The green and orange QDs exhibit lower quenching because of the high barrier to holes in these QDs. This is schematically represented in Fig. 3. In contrast, Zheng *et.al* reported lifetime quenching

decrease with an increase in the bandgap of the QD [12]. The opposite trend reported here could be due to the deeper valence band maximum of the NiO nanoparticles, at -6.22 eV, as compared to -5.04 eV reported by Zheng *et. al* [12]. In a QLED device the barrier to holes injected into the blue QDs is much lower when the NiO nanoparticles are used as HTL. It is clear from Fig. 3 that for other smaller band gap QDs, the barrier to hole injections into the QDs is even lower or non-existent. So far, the reported inorganic HTLs for QLED devices provide a very high barrier to QDs, thus reducing the efficiency [2-4]. On the other hand, NiO nanoparticles with a deeper valence band maximum are a potential HTL that can inject holes into the QDs of different sizes more efficiently.

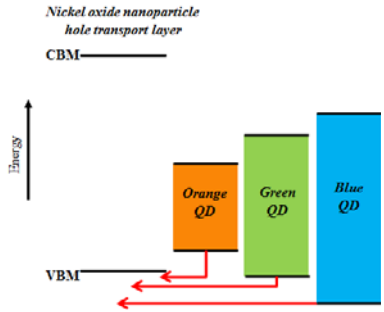

Figure 3. Schematic of the charge transport between 496 nm, 530 nm and 605 nm emitting QDs and the NiO nanoparticle hole transport layer. The holes in the larger QDs experience a larger barrier and hence their lifetime quench less than the smaller blue QDs.

CONCLUSION

In conclusion, near stoichiometric NiO nanoparticles are synthesized and characterized as a potential HTL for all-inorganic QLEDs. The NiO nanoparticles have a deeper valence band that aligns well with the QD valence bands for efficient charge injection. Moreover, the results indicate that NiO nanoparticles can inject carriers efficiently into different sized QDs.

REFERENCES

1. Y. Shirasaki, G. J. Supran, M. G. Bawendi, and V. Bulović, Nat. Phot. 7 (2013) 13-23.
2. J. M. Caruge, J.E. Halpert, V. Wood, V. Bulovic, and M. G. Bawendi, Nat. Phot. 2 (2008) 247-250.
3. B. S. Mashford, T. L. Nguyen, G. J. Wilson, and P. Mulvaney, J. Mater. Chem. 20 (2010) 167-172.
4. R. Vasan, H. Salman, and M. O. Manasreh, MRS Adv. 1 (2016) 305-310.
5. Bae, W. K., Char, K., Hur, H., & Lee, S., 20 (2008), 531–539.
6. B. Omogo, F. Gao, P. Bajwa, M. Kaneko, C. D. Heyes, ACS Nano 10 (2016) 4072-4082.
7. N. Durisic, A.G. Godin, D. Walters, P. Grutter, P. W. Wiseman, C. D. Heyes, ACS Nano 5 (2011), 9062-9073.
8. F. Gao, A. Kreidermacher, I. Fritsch, C. D. Heyes, Anal. Chem. 85 (2013) 4414-4422.

9. J. R. Manders, S. W. Tsang, M. J. Hartel, T. H. Lai, S. Chen, C. M. Amb, J. R. Reynolds, and F. So, Adv. Func. Mat. 23 (2013) 2993-3001.
10. S. Liu, R. Liu, Y. Chen, S. Ho, H. Jong, J. H. Kim, and F. So, Chem. Mater. 26 (2014) 4528-4534.
11. R. Srnbnek, I. Hotovy, V. Malcher, A. Vincze, D. McPhail, and S. Littlewood, IEEE ASDAM (2000) 303 – 306.
12. K. Zheng, K. Žídek, M. Abdellah, W. Zhang, P. Chábera, N. Lenngren, A. Yartsev, and T. Pullerits, J. Phys. Chem. 118 (2014) 18462-18471.